Structural basis and evolutionary origin of actin filament capping by twinfilin

Ville O Paavilainen, Maarit Hellman, Emmanuèle Helfer, Miia Bovellan, Arto Annila, Marie-France Carlier, Perttu Permi, Pekka Lappalainen

Structural basis and evolutionary origin of actin filament capping by twinfilin

Ville O. Paavilainen*†, Maarit Hellman‡, Emmanuèle Helfer†, Miia Bovellan*, Arto Annila‡, Marie-France Carlier†, Perttu Permi‡§, and Pekka Lappalainen*§

Programs in *Cellular Biotechnology and ‡Structural Biology and Biophysics, Institute of Biotechnology, University of Helsinki, FI-00014, Finland; and †Cytoskeleton Dynamics and Motility, Laboratoire d'Enzymologie et Biochimie Structurale, Centre National de la Recherche Scientifique, 91118 Gif-sur-Yvette, France

Edited by Thomas D. Pollard, Yale University, New Haven, CT, and approved December 16, 2006 (received for review October 3, 2006)

Dynamic reorganization of the actin cytoskeleton is essential for motile and morphological processes in all eukaryotic cells. One highly conserved protein that regulates actin dynamics is twinfilin, which both sequesters actin monomers and caps actin filament barbed ends. Twinfilin is composed of two ADF/cofilin-like domains, Twf-N and Twf-C. Here, we reveal by systematic domain-swapping/inactivation analysis that the two functional ADF-H domains of twinfilin are required for barbed-end capping and that Twf-C plays a critical role in this process. However, these domains are not functionally equivalent. NMR-structure and mutagenesis analyses, together with biochemical and motility assays showed that Twf-C, in addition to its binding to G-actin, interacts with the sides of actin filaments like ADF/cofilins, whereas Twf-N binds only G-actin. Our results indicate that during filament barbed-end capping, Twf-N interacts with the terminal actin subunit, whereas Twf-C binds between two adjacent subunits at the side of the filament. Thus, the domain requirement for actin filament capping by twinfilin is remarkably similar to that of gelsolin family proteins, suggesting the existence of a general barbed-end capping mechanism. Furthermore, we demonstrate that a synthetic protein consisting of duplicated ADF/cofilin domains caps actin filament barbed ends, providing evidence that the barbed-end capping activity of twinfilin arose through a duplication of an ancient ADF/cofilin-like domain.

ADF/cofilin | cytoskeleton | NMR

Eukaryotic cells rely on the actin cytoskeleton for performing vital cellular processes including motility, morphogenesis, endocytosis, and cytokinesis. During these processes, the structure and dynamics of the actin cytoskeleton are tightly controlled by a large number of actin-regulating proteins (1–4). Among the central cytoskeletal regulators are the gelsolin superfamily proteins, which control actin organization by severing filaments and by capping their barbed ends. These proteins are composed of either three or six homologous repeats of the gelsolin domain (G). Gelsolin is a calcium-regulated protein that contains six gelsolin domains (G1–G6) (5–7), arranged in a compact structure in the absence of Ca^{2+} (8). After binding to calcium, gelsolin is activated to expose the actin-binding surfaces on G1, G2, and G4 and to sever and cap filaments (9). Deletion studies have demonstrated that the minimal actin filament-capping region of gelsolin consists of domains G1 and G2 (10).

The ADF-H (actin-depolymerizing-factor homology) domain is a ubiquitous actin-binding motif (11). Despite the lack of detectable sequence homology, this domain shows clear structural similarity to the repeated domains of gelsolin (12). ADF-H domains also interact with actin through a similar interface to the gelsolin domains (13–15). The founding member of this family, ADF/cofilin, is entirely composed of one ADF-H domain that binds both actin monomers and filamentous actin and promotes rapid actin filament turnover by depolymerizing actin filaments from their pointed ends (16, 17).

Twinfilin is a conserved protein composed of two ADF-H domains, separated by an ≈30-residue linker region and followed by an ≈35-residue C-terminal tail region (18). Twinfilin promotes rapid actin filament turnover in cortical actin patches of budding yeast (19, 20), contributes to various actin-dependent developmental processes in *Drosophila* (21), and is involved in endocytosis in cultured mammalian cells (22, 23). Twinfilin binds ADP–G-actin in a 1:1 stoichiometric ratio and prevents actin filament assembly (18, 23). Both isolated ADF-H domains of twinfilin bind ADP–G-actin, but the high-affinity ADP–G-actin-binding site is located in the C-terminal ADF-H domain (24). Twinfilin also binds heterodimeric capping protein by means of its conserved C-terminal tail region, and this interaction is required for the correct subcellular localization of twinfilin, at least in budding and fission yeasts (25–27). Recent studies revealed that twinfilin, but not its isolated N- and C-terminal ADF-H domains, also caps filament barbed ends with preferential affinity for ADP-bound ends (23). Yeast twinfilin can induce filament severing at low pH (20). Thus, in addition to monomer sequestering, twinfilin displays similar activities to the gelsolin superfamily proteins.

Here, we show that unaltered actin-binding properties of both ADF-H domains are required for barbed-end capping by twinfilin and that each of the two domains plays a functionally and structurally distinct role in barbed-end capping. Combination of NMR studies, mutagenesis analyses, and functional biochemical and biomimetic motility assays revealed that the specific roles of these domains arise from structural differences and distinct actin-binding interfaces. We also provide evidence that the barbed-end capping proteins twinfilin and gelsolin evolved through independent domain duplications from ancient ADF/cofilin and gelsolin-like proteins, respectively.

Results

Twinfilin's C-Terminal ADF-H Domain Is Structurally Homologous to ADF/Cofilin. Twinfilin possesses two actin-binding domains, but only the structure of the isolated "low-affinity" N-terminal ADF-H domain (Twf-N) has been reported (28). Here, we used NMR spectroscopy to determine the structure of twinfilin's C-terminal, "high-affinity," ADF-H domain (Twf-C), consisting of residues

Author contributions: V.O.P. and M.H. contributed equally to this work; V.O.P., M.H., E.H., A.A., M.-F.C., P.P., and P.L. designed research; V.O.P., M.H., E.H., and M.B. performed research; V.O.P. and M.B. contributed new reagents/analytic tools; V.O.P., M.H., E.H., M.B., M.-F.C., P.P., and P.L. analyzed data; and V.O.P., M.H., E.H., A.A., M.-F.C., P.P., and P.L. wrote the paper.

The authors declare no conflict of interest.

This article is a PNAS direct submission.

Data deposition: The atomic coordinates of the C-terminal domain of twinfilin have been deposited in the Protein Data Bank, www.pdb.org (PDB ID code 2HD7).

§To whom correspondence may be addressed at: Institute of Biotechnology, P.O. Box 56, University of Helsinki, FI-00014 Helsinki, Finland. E-mail: pekka.lappalainen@helsinki.fi or perttu.permi@helsinki.fi.

This article contains supporting information online at www.pnas.org/cgi/content/full/0608725104/DC1.

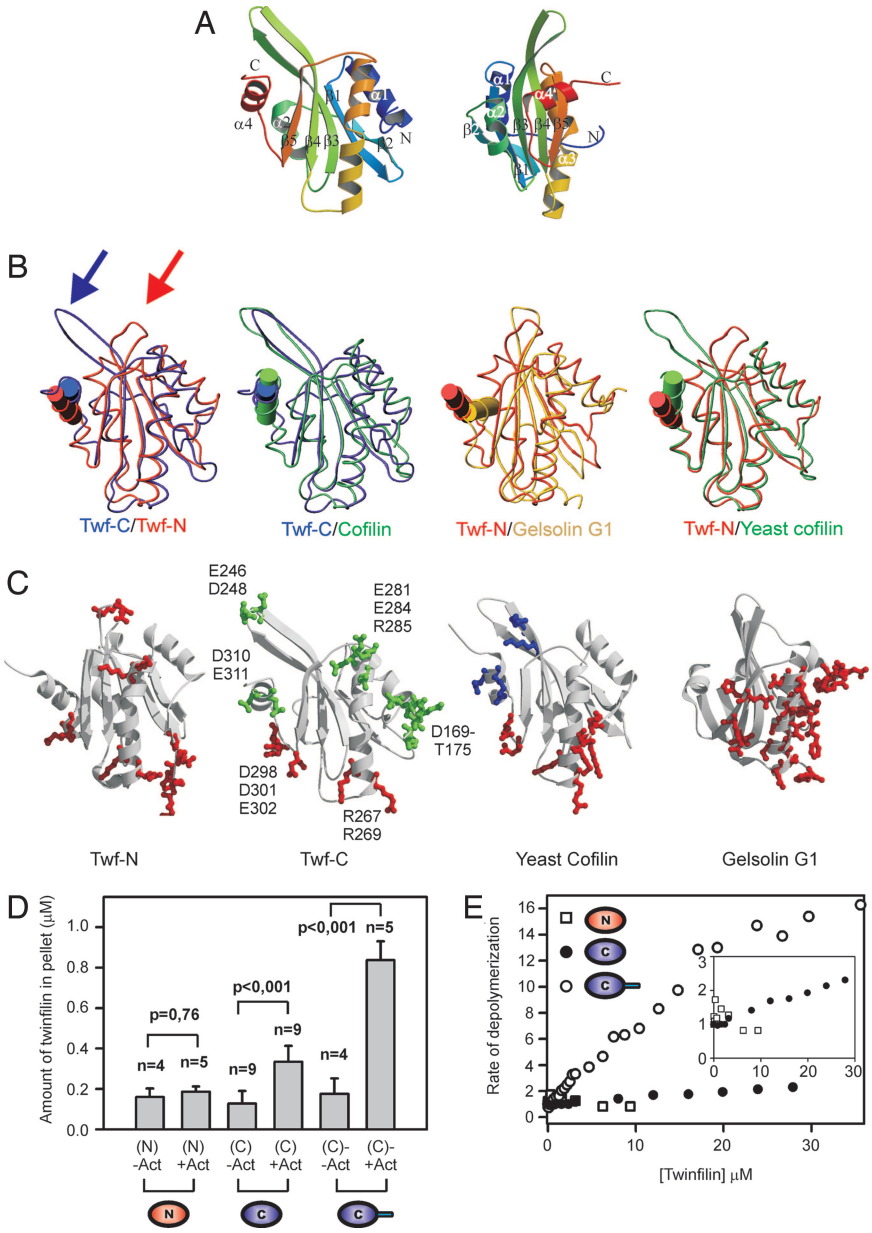

Fig. 1. Twinfilin's C-terminal ADF-H domain is structurally and functionally homologous to ADF/cofilin. (*A*) Schematic ribbon representation of the overall fold of Twf-C at two orientations rotated by 90°. The sequence is color coded from N to C terminus with blue through yellow to red. (*B*) A Cα-superimposition of Twf-C with Twf-N (28) (PDB ID code 1M4J) and yeast cofilin (32) (PDB ID code 1COF) and Twf-N with gelsolin segment-1 (PDB ID code 1D0N) and yeast cofilin. The β-strands 3 and 4 are oriented differently in Twf-N (red arrow) and Twf-C (blue arrow). (*C*) Ribbon diagrams of twinfilin$_{1–142}$, twinfilin$_{176–316}$, yeast cofilin, and gelsolin segment 1. The side chains of the residues important for actin-monomer binding are indicated in red. The side chains important for actin-filament binding are indicated in blue, and the Twf-C residues mutated in this study that do not contribute to actin-monomer binding are indicated in green. The Twf-C residues mutated in this study are indicated by letters and numbers (see SI Fig. 6 for the data). The residues important for actin binding in Twf-N cofilin and gelsolin segment 1 are from refs. 13, 28, and 46. (*D*) The amount of Twf-N or Twf-C (5 μM) cosedimenting with 10 μM actin filaments was determined. Twf-N does not shift to the pellet fraction upon addition of F-actin, whereas Twf-C cosediments with F-actin. The C-terminal tail region increases the affinity of Twf-C for F-actin. (*E*) Actin filament pointed-end depolymerization assay. 3 μM gelsolin-capped 50% pyrene-labeled actin filaments were diluted to 0.11 μM, and the rate of depolymerization was plotted at different twinfilin domain concentrations. Twinfilin's N-terminal ADF-H domain does not induce filament depolymerization, whereas the construct containing twinfilin's C-terminal ADF-H domain and the tail region increases the pointed-end depolymerization rate by ≈15-fold. Twinfilin's C-terminal ADF-H domain without the tail region increases pointed-end depolymerization by ≈2.5-fold (*Inset*).

176–316. Twf-C displays well dispersed NMR spectra with uniform signal intensities. Twf-C appears as a monomer according to its gel-filtration profile and the NMR relaxation data. Some dimerization and aggregation appeared when longer protein constructs were studied (data not shown).

A total of 3,112 nuclear Overhauser effect (NOE)-derived distance restraints were used for structure calculations [see supporting information (SI) Table 2]. With the exception of five first residues, the structure is well ordered throughout the sequence (SI Fig. 5). Twf-C possesses a typical ADF-H domain fold (Fig. 1*A*, SI Fig. 5). Structural alignment with the program Dali (29) showed significant similarities to structures of yeast cofilin (1cfy) (30) (Z score 16.3, rmsd 2.5 Å), glia maturation factor-β (1v6f) (Z score 14.8, rmsd 2.2 Å), mouse coactosin (31) (1wm4) (Z score 12.9, rmsd 3.0 Å), mouse Twf-N (1m4j) (28) (Z score 12.4, rmsd 2.9 Å), horse plasma gelsolin segment-1 (1d0n) (8) (Z score 6.1, rmsd 3.4 Å), and gelsolin segment 4 (Z score 5.9, rmsd 3.0 Å).

Within the ADF-H domain protein family, the β-extension formed by β3- and β4-sheets can adopt different orientations (28, 31–33). This region is critical for actin filament binding of different ADF-H domain proteins (13, 33, 34). Importantly, in twinfilin's N-terminal domain, which was reported to bind only G-actin, the orientation of this β-extension is different from other ADF-H domains. Whereas the long β-extension in F-actin binding ADF/cofilins and coactosins protrudes away from the main protein body, this region is tilted toward the C-terminal end of the helix α3 in Twf-N (28). When an ADF/cofilin is replaced by Twf-N in the currently available F-actin-binding model (15), the strands β3 and β4 in Twf-N point toward the actin filament, causing a steric hindrance and thus providing a possible explanation for the differences in actin interactions (monomer vs. filament binding) between different ADF-H domains.

Interestingly, the β3–β4-extension has the same orientation in F-actin-binding ADF/cofilins and Twf-C and a significantly different orientation in Twf-N, suggesting that Twf-C may display F-actin-binding activities similar to those of ADF/cofilin (Fig. 1*B*). The β3-β4 extension of Twf-C is relatively rigid, as determined by the ^{15}N T_1 and T_2 relaxation time measurements (data not shown)

and the low rmsd value between the ensemble of structures. In addition, the C-terminal helix (α4) in Twf-C has the same orientation as in yeast cofilin (indicated by cylinders in Fig. 1*B*), with a difference of ≈28° relative to the helix axes. The spatial and angular orientations of the C-terminal helix of Twf-N are clearly different.

To map the G-actin-binding interface of Twf-C, we generated six mutations in this domain and assayed the mutated proteins for ADP–G-actin binding. Five mutations were alanine substitutions of residues corresponding to the G- or F-actin-binding regions of ADF/cofilin and Twf-N (13, 28). The sixth mutation was a deletion of the disordered N terminus of Twf-C (residues Asp-169–Gly-177). The affinities of the mutant proteins for ADP–G-actin under physiological ionic conditions were determined by measuring the change in the fluorescence of NBD-labeled Mg-ADP–G-actin (24). Mutants E246A, D248A; E281A, E284A, R285A; D310A, E311A and the N-terminal deletion yielded K_D values very similar to the one of wild-type Twf-C (≈20 nM). Mutations D298A,D301A, E302A, and R267A,R269A displayed significantly reduced affinities for ADP–G-actin (K_D 246 nM and not detectable, respectively) (SI Fig. 6). In the 3D structure of Twf-C, the mutations that impair binding to actin are located within a surface that resembles the surface of ADF/cofilin that appears essential for G- and F-actin binding (13). In contrast, the previously determined G-actin-binding site of Twf-N is different and more extended as compared with the G-actin-binding sites of Twf-C and yeast cofilin (28). In conclusion, Twf-C interacts with actin through an interface similar to that for ADF/cofilin (Fig. 1*C*).

Twf-C Binds F-Actin in an ADF/Cofilin-Like Mechanism. To examine whether Twf-C binds F-actin like ADF/cofilin, we performed F-actin cosedimentation assays. Twf-C, but not Twf-N, cosedimented with F-actin. This assay also revealed that twinfilin's C-terminal tail region increased the affinity of Twf-C to F-actin (Fig. 1*D*). We next examined whether Twf-C could also increase filament pointed-end depolymerization like ADF/cofilin. The initial rate of dilution-induced depolymerization of gelsolin-capped filaments increased by ≈2.5-fold on increasing Twf-C concentration but was unaffected by Twf-N. The presence of the C-terminal tail resulted in a further increase in F-actin depolymerization from the pointed ends, consistent with the results of the cosedimentation assay (Fig. 1*E*). Together, these results revealed that, whereas Twf-N binds only actin monomers, Twf-C binds also to the sides of F-actin filaments in a mechanism functionally similar to ADF/cofilin.

The Presence of the Two ADF-H Domains in Fully Functional State Is Necessary for Barbed-End Capping by Twinfilin. We next examined the roles of twinfilin's two ADF-H domains in ADP-G-actin binding and filament barbed-end capping by a systematic domain-swapping/inactivation analysis. A similar study has been carried out on gelsolin family proteins to determine the functions of their individual domains (10, 35). Six mutant proteins (Table 1) were constructed by swapping the order of either the N-terminal (residues 1–142) or C-terminal (residues 169–316) ADF-H domains, by generating proteins with two N- or C-terminal domains, by deleting the C-terminal tail-region, or by specifically inactivating either one of the domains by point mutations known to abolish their ability to bind ADP-G-actin (R96A,K98A in Twf-N, R267A,R269A in Twf-C) (ref. 28 and this study). It is important to note that the positions of the linker region and the C-terminal tail were retained in these constructs.

In an NBD-actin fluorescence assay, all mutants bound Mg-ADP-G-actin with relatively high affinity (K_D values ≈45–500 nM) (Fig. 2*A*, SI Fig. 7*A*, and Table 1). As expected, the proteins composed of two Twf-N domains (N-N mutant) or harboring an inactivated Twf-C domain behaved like the Twf-N domain, i.e., bound actin with lower affinity than Twf-C (24) and induced a decrease in the NBD-actin fluorescence (24). Furthermore, the mutated protein containing two Twf-C domains (C-C mutant) bound two G-actin molecules, whereas wild-type twinfilin binds G-actin with a 1:1 stoichiometry (SI Fig. 7*B*). This assay demonstrated that neither the correct composition nor the order of twinfilin's ADF-H domains is critical for G-actin binding (Table 1).

Table 1. A schematic representation of twinfilin domain-swapping/inactivation mutant proteins used in this study

Protein construct	Biochemical properties: ADP–G-actin binding, μM	Barbed-end capping, μM	Bead motility
	0.043	0.2 (23)	+++
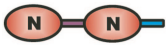	0.197	n.d.	+
	0.023	0.01	+++
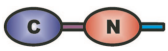	0.054	0.21	+++
	0.202	4.69	++
	0.129	n.d.	−
	0.582	n.d.	−
	0.700 (24)	n.d. (23)	−
	0.060 (24)	n.d. (23)	+

The affinities of the proteins to Mg-ADP–G-actin at physiological ionic conditions was measured by NBD-actin fluorescence assay (Fig. 2 and SI Fig. 7). The actin filament barbed-end capping affinity (K_F) was measured by pyrene-actin polymerization assays (Fig. 2 and SI Fig. 8). Filament barbed-end capping was also evaluated by a biomimetic bead motility assay (Fig. 2 and SI Fig. 9). No detectable activity is indicated by n.d.

Barbed- and pointed-end growth assays were carried out in the presence of the aforementioned mutant proteins as described (23). Twinfilin inhibits pointed-end growth by simple sequestration, whereas it prevents barbed-end assembly by both sequestering actin monomers and capping filament ends (23). The C-C and C-N mutant proteins displayed barbed-end capping activity like wild-type twinfilin (K_F values 0.01 μM and 0.21 μM, respectively, versus 0.2 μM for wild-type protein). In contrast, the mutant proteins containing two N-terminal ADF-H domains or inactivated N- or C-terminal domains did not display detectable barbed-end capping activity (Fig. 2*B*, Table 1, and SI Fig. 8). Deletion of the C-terminal tail significantly reduced capping activity (K_F = 4.69 μM), consistent with data in Fig. 1. Thus, Twf-C, together with the tail region, plays a crucial role in barbed-end capping.

The barbed-end capping activities of the mutant proteins were further tested in a biomimetic motility assay (36). Barbed-end cappers are required for motility, hence this assay can be used to challenge the barbed-end capping activity of a protein of interest (36, 37). N-WASP-coated beads were placed in a motility medium containing actin, Arp2/3, ADF, and profilin as well as 0.5 μM wild-type or mutant twinfilins as the barbed-end capper. The C-C, C-N, and N-C mutants induced formation of actin tails and promoted motility of the beads, indicating that these twinfilin variants capped barbed ends like wild-type twinfilin. The mutants with inactivated N- or C-terminal ADF-H domains did not promote motility (Table 1, Fig. 2*C*, SI Fig. 9, and SI Movies 1–3). These results are in agreement with polymerization assays. However, at variance with the polymerization assays, slow motility and poor actin tail formation was observed with the N-N mutant, indicating very weak barbed-end capping by this mutant. The weak barbed-

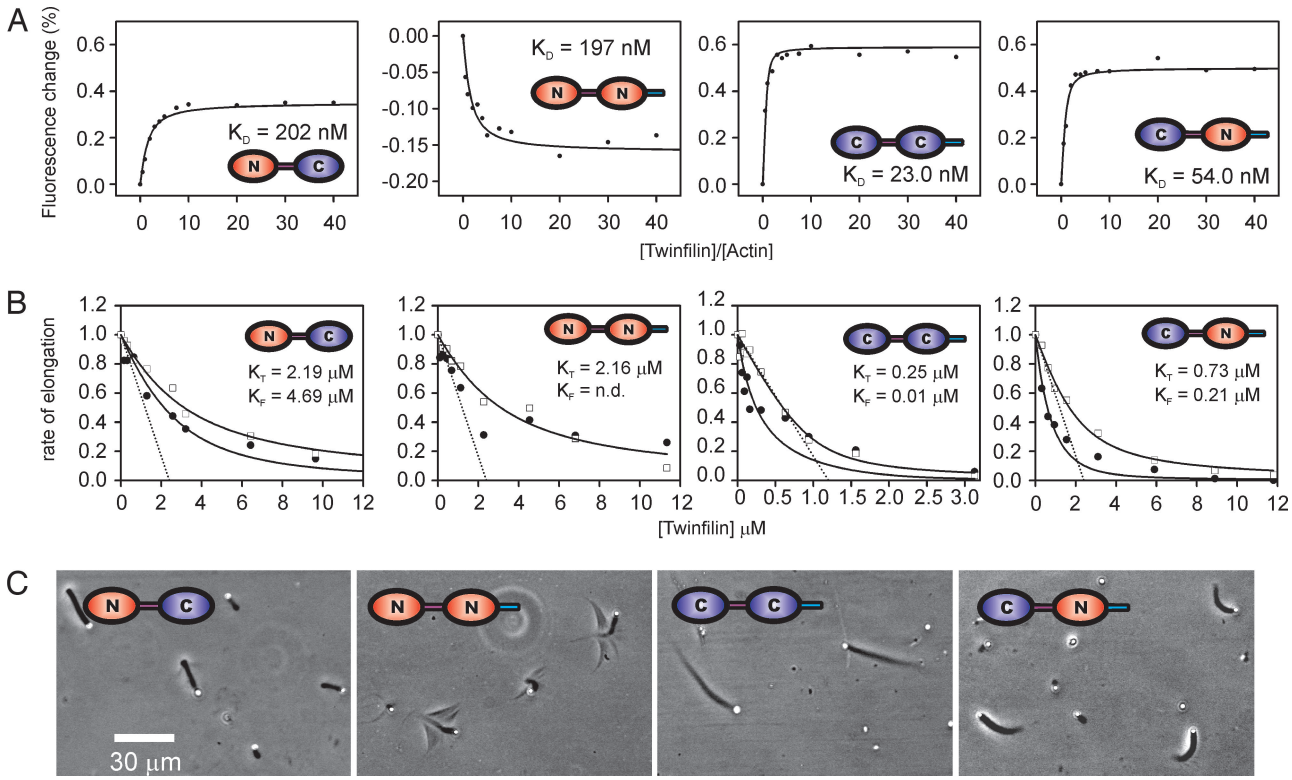

Fig. 2. Interaction of twinfilin domain-swap mutants with G-actin and filament barbed ends. (*A*) The change in the fluorescence of NBD-labeled Mg-ADP–G-actin was measured at different concentrations of the mutant proteins. Symbols indicate data, and solid lines indicate fitted binding curves for a complex with 1:1 stoichiometry (1:2 stoichiometry for the C-C mutant). (*B*) The F-actin capping activity of the domain-swap mutants measured by a pyrene–actin polymerization assay. Barbed-end growth (filled circles) and pointed-end growth (open squares) were initiated by using spectrin–actin seeds and gelsolin–actin seeds, respectively, in the presence of 2.5 μM G-actin (10% pyrenyl-labeled) and twinfilin as indicated. The initial rates were normalized to the value of 1 measured in the absence of twinfilin. Similarly to wild-type twinfilin (23) the inhibition of barbed-end polymerization was stronger at low concentrations of C-C, C-N, and N-C constructs than expected from monomer sequestering, indicating barbed-end capping. In contrast, the protein composed of two N-terminal domains did not cap barbed ends based on this assay. The obtained K_T (ATP–G-actin sequestration) and K_F values (barbed-end capping) are depicted in the figure. (*C*) The abilities of the mutant proteins to replace capping protein in a biomimetic motility assay were tested. Wild-type twinfilin as well as C-C, C-N, and N-C constructs rescued the tail morphology and bead motility. Also the N-N mutant was partially capable in rescuing bead motility, although the morphology of actin tails was severely abnormal in the presence of this mutant.

end-capping activity of the N-N mutant probably results from an interaction of Twf-N with the terminal actin monomers at the barbed end, because Twf-N did not compete with Twf-C for F-actin binding (data not shown), increased bead motility in the presence of suboptimal concentration of wild-type twinfilin (SI Fig. 10*A*), and increased the weak bead motility induced by very high concentrations (15 μM) of Twf-C (SI Fig. 10*B*).

Finally, we addressed the role of twinfilin's linker region in filament barbed-end capping. Deletion analysis demonstrated that the length of the linker can be reduced from 26 residues (in wild-type twinfilin) to 17 residues without significantly inhibiting barbed-end capping. Further deletion to 7 or 1 residues abolished barbed-end capping activity, whereas the ADP-G-actin binding was maintained with unchanged affinity (SI Fig. 11).

These data suggest that the twinfilin's C-terminal ADF-H domain (and its tail region) provides the main actin-binding element in barbed-end capping by binding to the side of the F-actin terminal subunit, whereas the N-terminal ADF-H domain interacts differently with the F-actin terminal subunit.

Engineering ADF/Cofilin into a Filament Barbed-End Capping Protein. The assays described above confirm and expand the conclusion (23) that the two functional ADF-H domains are required for efficient barbed-end capping by twinfilin and that at least one of these domains must have capacity to bind G- and F-actin. To test this hypothesis, we constructed a hybrid protein in which two ADF/cofilins were joined together by a linker region from twinfilin (to yield a cof-cof protein). Mouse cofilin-2 was chosen for this construct, because of its relatively weak F-actin depolymerization activity and high affinity for G- and F-actin (38). The purified cof-cof protein was fully soluble and monomeric and bound ADP-G-actin with an affinity of ≈5 nM, assuming a binding stoichiometry of 1:2 (SI Fig. 12*A*). The cof-cof protein displayed strong inhibition of growth at both ends, with more efficient (higher affinity) inhibition at the barbed end, suggestive of barbed-end capping like twinfilin (SI Fig. 12*B*). In a biomimetic motility assay, the cof-cof protein was capable of replacing a barbed-end-capping protein in promoting actin tail formation and bead motility with an optimal cof-cof concentration of ≈0.2 μM (Fig. 3 *A* and *B*). Importantly, 0.2 μM purified cofilin-2 did not promote actin tail formation or bead motility, whereas 0.1 μM cof-cof promoted bead motility. In conclusion, the two interconnected ADF-H domains of the synthetic cof-cof protein are sufficient to generate a barbed-end-capping activity.

Discussion

This work has focused on the structural basis of the barbed-end-capping activity of mammalian twinfilin (23). The capping activity of twinfilin had been shown to require the two ADF-H domains of the protein, each individual domain harboring only a G-actin-sequestering activity (23, 24). Now, we show that the two ADF-H domains of twinfilin display different structures and actin-binding

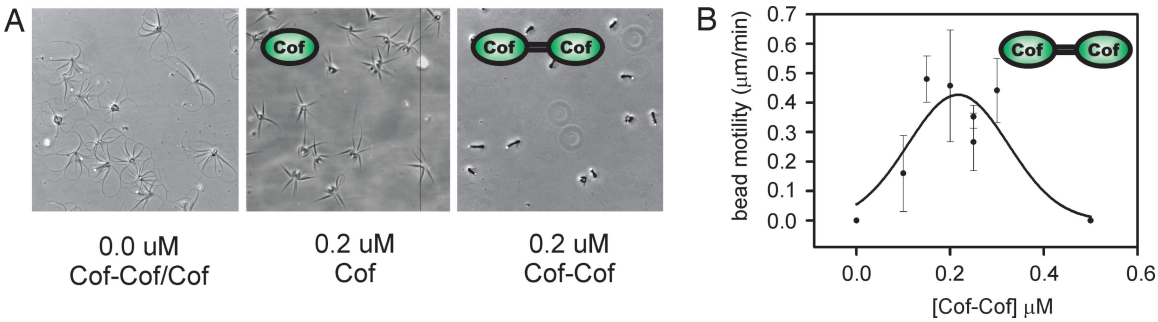

Fig. 3. A hybrid protein composed of two ADF/cofilins fused together by twinfilin's linker region caps actin-filament barbed ends. (*A*) The effects of 0 μM or 0.2 μM cofilin-2, and 0.2 μM cof-cof mutant on the bead motility in the absence of barbed-end capper. Addition of the cof-cof mutant, but not wild-type cofilin-2, restores actin tail formation and bead motility, confirming barbed-end capping by cof-cof. (*B*) Quantification of bead velocities at various cof-cof concentrations. The data are average velocities of at least 10 beads and their standard deviations.

interfaces and that these features are essential in filament barbed-end capping. We further show that (*i*) the order and the composition of the ADF-H domains are not critical for twinfilin's actin monomer binding activities; (*ii*) twinfilin's C-terminal ADF-H domain is structurally and functionally homologous to ADF/cofilins, in binding both monomeric and filamentous actin and increasing the rate of pointed-end depolymerization; (*iii*) twinfilin's isolated N-terminal ADF-H domain binds only monomeric actin with detectable affinity and is structurally homologous to gelsolin segment 1; (*iv*) unaltered actin binding of both ADF-H domains is required for barbed-end capping by twinfilin; and (*v*) a twinfilin-like filament barbed-end-capping protein can be engineered by joining two ADF/cofilins together with an appropriate linker.

The ADF/cofilin-like fold of twinfilin's C-terminal ADF-H domain provides a possible structural explanation for its observed filament side-binding and pointed-end depolymerization activities. The previously determined structure of twinfilin's N-terminal domain (28), on the other hand, displays a different orientation of β-sheets 3 and 4 as compared with other F-actin binding ADF-H domains or Twf-C. It was proposed that this structural difference may account for the inability of Twf-N to bind F-actin (28). Strikingly, the orientation of β-sheets 3 and 4 in Twf-N is very similar to the homologous region of gelsolin segment 1. These data lead us to consider a comprehensive structural model for barbed-end capping by modular proteins like twinfilin and gelsolin, as follows.

Twinfilin's ADF-H domains are structurally related to the six gelsolin domains (Figs. 1 and 4), sharing highest similarity with gelsolin domains 1, 2, 4, and 5. ADF-H and gelsolin domains are believed to bind actin through a similar interface (15, 39). Gelsolin domains 1 and 2 (G1 and G2) constitute the minimal region capable of capping actin filament barbed ends (10). Analogous to twinfilin's N-terminal domain, gelsolin domain G1 binds actin monomers, whereas G2 contains filament-binding activity like twinfilin's C-terminal domain. A structural model for actin filament capping by gelsolin fragment G1-G2 was recently prepared from the G1-G3/G-actin cocrystal structure (40). The obtained biochemical and structural data, combined with the similarities in the binding mode of G1-G2 and twinfilin to F-actin (40), enabled us to build a schematic model of the twinfilin-capped actin filament barbed end (Fig. 4 and SI Movie 4). The model was constructed by superimposing the structure of twinfilin's N-terminal ADF-H domain (PDB ID code 1M4J) on the gelsolin segment 1 bound to the terminal actin monomer in the G1-G3/actin structure (PDB ID code 1RGI). The orientation of twinfilin was also nearly identical when ADF/cofilin was replaced by Twf-N in a molecular dynamics simulation model of cofilin/G-actin complex (15). The C-terminal twinfilin domain (PDB ID code 2HD7) was then positioned based on the G2 in the G1-G3-actin model (40), and this orientation was in good agreement with the mutagenesis results from this work. However, it is important to note that, although Twf-N shows high structural similarity to G1, Twf-C is structurally less homologous to G2.

The obtained model of a twinfilin-capped barbed end also demonstrated that twinfilin's C-terminal ADF-H domain can be placed either to the side of the filament or to the terminal actin monomer without a steric hindrance. This finding is in line with the biochemical data showing that the mutant protein composed of two C-terminal ADF-H domains efficiently caps filament barbed ends. In contrast, the N-terminal domain (PDB ID code 1M4J) can be placed only on the terminal actin monomer. Superimposing this domain with the gelsolin segment-2 causes a steric hindrance between the actin filament and the extension formed by β-sheets 3 and 4 of the N-terminal domain. This model agrees with the obtained biochemical data and provides a structural explanation for the distinct biochemical and structural roles of twinfilin's two ADF-H domains during filament barbed-end capping. The proposed model for twinfilin capping is based on two other structural models, and thus further work is required to reveal the exact molecular mechanism of this interaction. Furthermore, the exact structural role of twinfilin's linker region and possible sequence-

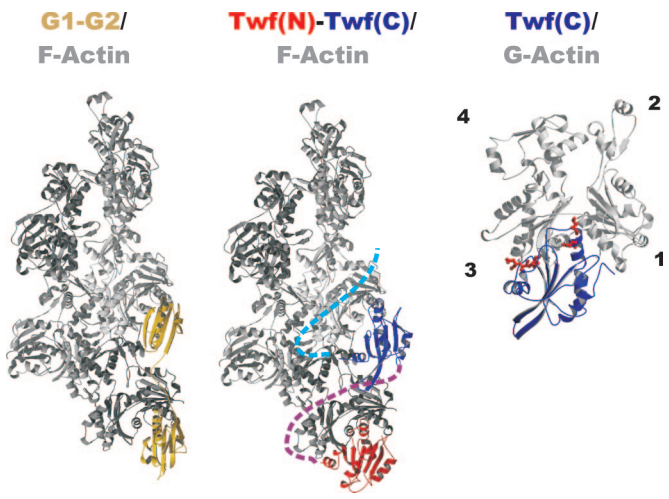

Fig. 4. A schematic model of gelsolin G1-G2- and twinfilin-capped actin filament barbed ends. (*Left*) The Holmes model of an actin filament (47) with G1-G2 from the G1-G3 actin monomer structure fitted onto the barbed end as presented in ref. 40. (*Center*) Schematic presentation of twinfilin's binding to F-actin is derived from the gelsolin-G-actin structure, gelsolin-F-actin and ADF/cofilin-G-actin models, and the mutagenesis data from this study for Twf-C and from ref. 28 for Twf-N. (*Right*) A model of interaction of twinfilin's ''high-affinity'' C-terminal ADF-H domain with actin monomer. The residues critical for G-actin binding identified in this study are highlighted in red.

specific interactions between the linker and actin in barbed-end capping remain to be determined.

Phylogenetic analyses demonstrated that twinfilin arose through a domain duplication from an ancestral ADF/cofilin-like protein (11). The data presented here suggest that this domain duplication led to the emergence of an ancient twinfilin that bound actin monomers similarly to its ancestor, but simultaneously also gained a filament barbed-end capping activity. This domain duplication may also have simultaneously led to an evolution of filament-severing activity at low pH (20). This evolutionary scheme is supported by our data showing that an ADF/cofilin can be engineered into a twinfilin-like barbed-end capping protein through domain duplication. According to this scheme, twinfilin's N-terminal ADF-H domain evolved further to allow binding only to G-actin or filament ends, thus targeting twinfilin to filament barbed ends.

The evolution of gelsolin proceeded through analogous domain duplications to generate an actin filament-capping/severing protein (41). Interestingly, gelsolin domains and ADF-H domain proteins do not show detectable sequence homology to each other, demonstrating that the domain duplications in gelsolin and ADF/cofilin lineages occurred independently. Later, these two proteins gained additional functions in their lineages (e.g., interaction with heterodimeric capping protein by twinfilin and calcium regulation of gelsolin). The presence of two structurally homologous domains/subunits appears to be a common theme among all filament barbed-end cappers characterized so far, with the possible exception of Eps8 (37). Capping protein (CapZ and its homologues) is a heterodimer composed of two structurally homologous subunits (42, 43); formins are homodimers (44), and gelsolin, twinfilin, and the engineered cof-cof are composed of (at least) two structurally homologous actin-binding domains (ref. 40 and this study). However, although the individual domains of twinfilin and gelsolin are capable of binding G-actin, this has not been demonstrated for other barbed-end-capping proteins described above.

In summary, the two ADF-H domains of twinfilin are structurally and functionally different from each other and evolved to play distinct roles during filament barbed-end capping. The structural and functional similarity of the two ADF-H domains to the two first domains of gelsolin (G1 and G2) suggested a common molecular model for filament barbed-end capping by twinfilin and gelsolin. This proposal must now be challenged by the structural analysis of the twinfilin–actin or ADF/cofilin–actin complexes.

Methods

Biochemical Assays. The affinities for wild-type and mutant twinfilin's for ADP-actin monomers were determined by measuring the change in the fluorescence of NBD-labeled G-actin as described (24). Actin assembly was monitored by the increase in the fluorescence of 2.5 μM 10% pyrenyl-actin (excitation and emission wavelengths of 366 and 407 nm, respectively). Barbed-end growth was monitored by using spectrin–actin seeds and pointed-end growth was monitored by using gelsolin–actin seeds. The ATP-actin sequestration and barbed-end capping were modeled as described (23). F-actin cosedimentation assays were performed with 10 μM F-actin and 5 μM twinfilin constructs as described (13). Cloning, expression, and purification of proteins are described in *SI Methods*.

Motility Assays. Motility assays were carried out as described (23, 45). The standard motility medium consisted of 7 μM F-actin, 9 μM ADF, 2.4 μM profilin, 90 nM gelsolin, and 90 nM Arp2/3. The steady state of actin assembly was reached in 10 min, after which Valap-sealed samples were observed in phase-contrast microscopy (AX70; Olympus, Melville, NY) equipped with a $\times$20 phase objective (NA 0.5), a motorized stage (Märzhäuser, Wetzlar–Steindorf, Germany) and a CCD camera (Cascade Photometrics, Tucson, AZ).

Miscellaneous. Cloning, protein expression and purification, and structure determination of Twf-C are described in *SI Methods*.

We thank Dominique Didry and Diep Le (Centre National de la Recherche Scientifique, Gif-sur-Yvette, France) for providing various proteins used in the assays. This study was supported by Academy of Finland Grants 106852 (to P.P.) and 205629 (to P.L.); the Sigrid Juselius Foundation (P.L.); the Ligue Nationale Contre le Cancer (M.-F.C. is Équipe Labellisée Ligue); Human Frontier Science Program Research Grant RGP0072/2003-C (to M.-F.C.); and the Kordelin Foundation and the French Embassy Science Council (V.O.P.).

1. Pollard TD, Blanchoin L, Mullins RD (2000) *Annu Rev Biophys Biomol Struct* 29:545–576.
2. Pantaloni D, Le Clainche C, Carlier MF (2001) *Science* 292:1502–1506.
3. Paavilainen VO, Bertling E, Falck S, Lappalainen P (2004) *Trends Cell Biol* 14:386–394.
4. Nicholson-Dykstra S, Higgs HN, Harris ES (2005) *Curr Biol* 15:R346–R357.
5. McGough AM, Staiger CJ, Min JK, Simonetti KD (2003) *FEBS Lett* 552:75–81.
6. Silacci P, Mazzolai L, Gauci C, Stergiopulos N, Yin HL, Hayoz D (2004) *Cell Mol Life Sci* 61:2614–2623.
7. Yin HL, Stossel TP (1979) *Nature* 281:583–586.
8. Burtnick LD, Koepf EK, Grimes J, Jones EY, Stuart DI, McLaughlin PJ, Robinson RC (1997) *Cell* 90:661–670.
9. Robinson RC, Mejillano M, Le VP, Burtnick LD, Yin HL, Choe S (1999) *Science* 286:1939–1942.
10. Way M, Pope B, Weeds AG (1992) *J Cell Biol* 119:835–842.
11. Lappalainen P, Kessels MM, Cope MJ, Drubin DG (1998) *Mol Biol Cell* 9:1951–1959.
12. Hatanaka H, Ogura K, Moriyama K, Ichikawa S, Yahara I, Inagaki F (1996) *Cell* 85:1047–1055.
13. Lappalainen P, Fedorov EV, Fedorov AA, Almo SC, Drubin DG (1997) *EMBO J* 16:5520–5530.
14. Van Troys M, Dewitte D, Verschelde JL, Goethals M, Vandekerckhove J, Ampe C (1997) *J Biol Chem* 272:32750–32758.
15. Wriggers W, Tang JX, Azuma T, Marks PW, Janmey PA (1998) *J Mol Biol* 282:921–932.
16. Carlier MF, Laurent V, Santolini J, Melki R, Didry D, Xia GX, Hong Y, Chua NH, Pantaloni D (1997) *J Cell Biol* 136:1307–1322.
17. Bamburg JR (1999) *Annu Rev Cell Dev Biol* 15:185–230.
18. Palmgren S, Vartiainen M, Lappalainen P (2002) *J Cell Sci* 115:881–886.
19. Goode BL, Drubin DG, Lappalainen P (1998) *J Cell Biol* 142:723–733.
20. Moseley JB, Okada K, Balcer HI, Kovar DR, Pollard TD, Goode BL (2006) *J Cell Sci* 119:1547–1557.
21. Wahlstrom G, Vartiainen M, Yamamoto L, Mattila PK, Lappalainen P, Heino TI (2001) *J Cell Biol* 155:787–796.
22. Pelkmans L, Fava E, Grabner H, Hannus M, Habermann B, Krausz E, Zerial M (2005) *Nature* 436:78–86.
23. Helfer E, Nevalainen EM, Naumanen P, Romero S, Didry D, Pantaloni D, Lappalainen P, Carlier MF (2006) *EMBO J* 25:1184–1195.
24. Ojala PJ, Paavilainen VO, Vartiainen MK, Tuma R, Weeds AG, Lappalainen P (2002) *Mol Biol Cell* 13:3811–3821.
25. Palmgren S, Ojala PJ, Wear MA, Cooper JA, Lappalainen P (2001) *J Cell Biol* 155:251–260.
26. Falck S, Paavilainen VO, Wear MA, Grossmann JG, Cooper JA, Lappalainen P (2004) *EMBO J* 23:3010–3019.
27. Kovar DR, Wu JQ, Pollard TD (2005) *Mol Biol Cell* 16:2313–2324.
28. Paavilainen VO, Merckel MC, Falck S, Ojala PJ, Pohl E, Wilmanns M, Lappalainen P (2002) *J Biol Chem* 277:43089–43095.
29. Holm L, Sander C (1998) *Nucleic Acids Res* 26:316–319.
30. Fedorov AA, Lappalainen P, Fedorov EV, Drubin DG, Almo SC (1997) *Nat Struct Biol* 4:366–369.
31. Hellman M, Paavilainen VO, Naumanen P, Lappalainen P, Annila A, Permi P (2004) *FEBS Lett* 576:91–96.
32. Fedorov AA, Ball T, Mahoney NM, Valenta R, Almo SC (1997) *Structure (London)* 5:33–45.
33. Quintero-Monzon O, Rodal AA, Strokopytov B, Almo SC, Goode BL (2005) *Mol Biol Cell* 16:3128–3139.
34. Ono S, McGough A, Pope BJ, Tolbert VT, Bui A, Pohl J, Benian GM, Gernert KM, Weeds AG (2001) *J Biol Chem* 276:5952–5958.
35. Yu FX, Zhou DM, Yin HL (1991) *J Biol Chem* 266:19269–19275.
36. Loisel TP, Boujemaa R, Pantaloni D, Carlier MF (1999) *Nature* 401:613–616.
37. Disanza A, Carlier MF, Stradal TE, Didry D, Frittoli E, Confalonieri S, Croce A, Wehland J, Di Fiore PP, Scita G (2004) *Nat Cell Biol* 6:1180–1188.
38. Vartiainen MK, Mustonen T, Mattila PK, Ojala PJ, Thesleff I, Partanen J, Lappalainen P (2002) *Mol Biol Cell* 13:183–194.
39. Dominguez R (2004) *Trends Biochem Sci* 29:572–578.
40. Burtnick LD, Urosev D, Irobi E, Narayan K, Robinson RC (2004) *EMBO J* 23:2713–2722.
41. Choe H, Burtnick LD, Mejillano M, Yin HL, Robinson RC, Choe S (2002) *J Mol Biol* 324:691–702.
42. Yamashita A, Maeda K, Maeda Y (2003) *EMBO J* 22:1529–1538.
43. Wear MA, Cooper JA (2004) *Trends Biochem Sci* 29:418–428.
44. Higgs HN (2005) *Trends Biochem Sci* 30:342–353.
45. Wiesner S, Helfer E, Didry D, Ducouret G, Lafuma F, Carlier MF, Pantaloni D (2003) *J Cell Biol* 160:387–398.
46. McLaughlin PJ, Gooch JT, Mannherz HG, Weeds AG (1993) *Nature* 364:685–692.
47. Holmes KC, Popp D, Gebhard W, Kabsch W (1990) *Nature* 347:44–49.